Society for Information Display 2017 (SID2017), USA, 21-26 May, 2017.

Reproduction of Perceptual Reality in Standard-Dynamic-Range (SDR) Environments Using High-Dynamic-Range (HDR) Images Compressed by Global Tone Mapping

Saki Iwaida*, Yoshitaka Fukaya*, Eri Irieda*, Tomomi Yamasaki*, Anis Ur Rehman**,
Ken Kihara*, Toshiki Iso***, Sakuichi Ohtsuka*

Abstract

In the real world, human observers perceive various objects under a wide range of luminance values from low to high [1]. Images that try to reproduce the same range end up looking overexposed, underexposed, or both. This is because our visual systems can capture a full range of tones in high contrast scenes. In order to display HDR images or videos, quite dark rooms are conventionally required to avoid the picture quality degradation caused by viewing flare from illumination in the room. The next step is therefore, converting HDR images/videos into Standard-Dynamic-Range (SDR) images/videos that retain their Perceptual Reality (PR), i.e., reducing the impairments caused by flare, for comfortably utilizing HDR contents in daily life often. Tone Mapping Operators (TMOs) are now being used to compress HDR into SDR images. However, there is no evidence that all the conditions, separately or jointly, provide satisfactory results from the human perspective.

Our physiological experiments in a real HDR environment confirmed that (1) most observers maybe able to judge the luminance differences in global luminance perception except for specific lighting cases, e.g., the object is to be viewed against a strong light-source like the sun, and (2) JND (Weber-ratio) in luminance perception increases, i.e., luminance sensitivity decreases, except for between highlight and middle tone in a scene.

Based on subjective assessments conducted in a real HDR environment, our proposal demonstrates that the global tone mapping technique is quite effective in reproducing HDR images (Contrast Ratio (CR) > 1000:1) in normal or SDR environments with typical viewing flare (CR < 20:1).

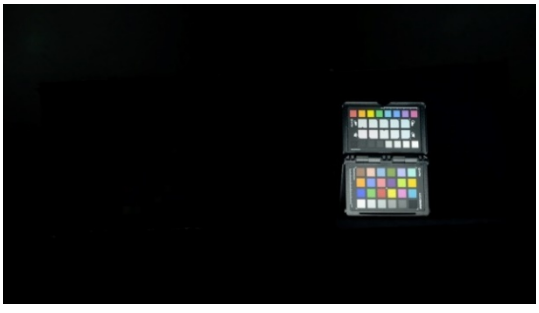

Figure1. Original HDR image

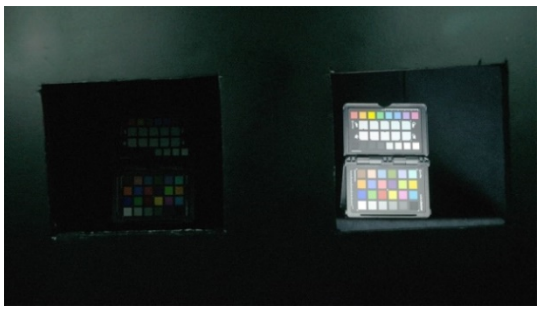

Figure2. SDR image by our proposal (CR < 20:1)

References

1) D. Nightingale: “Practical HDR: A complete guide to creating High Dynamic Range images with your digital SLR,” Focal Press, 2011.

* Graduate School of Science and Engineering, Kagoshima University, Kagoshima, Japan
** National Institute of Technology, Kagoshima College, Kagoshima, Japan
*** Research Laboratories, NTT DOCOMO, Inc., Kanagawa, Japan

21st International Conference on Circuits, Systems, Communications and Computers
July 14-17, 2017, Heraklion, Greece

Extraction of Human Stepping Pattern UsingAcceleration Sensors

Takayuki Toyohira[1], Kiminori Sato[1] and Mutsumi Watanabe[1]

Abstract

Gait pattern of person characterizes individual and each condition. The precise gait pattern may be one of the measures for recognizing individuals [1][2][3][4]. Gait analysis systems using acceleration sensor were developed for medical rehabilitation [5] and identification of portable device user [6], etc. However, most systems do not catch synchronous stepping actions between right foot and left foot. In this paper, a synchronous walking sensing system is developed, where a pair of acceleration and angular velocity sensors are attached to left and right shoes of a walking person and their data are transmitted to a PC through a wireless channel. Walking data from 19 students of the age of 14 to 20 are acquired for walking analysis.

In the sensor data, x and z components of accelerations and y component of acceleration are used for analysis of walking. Stepping time diagrams are extracted from the acquired data of right and left foot actions of stepping-off and -on the ground, and the time diagrams distinguish between an ordinary person and a person injured on left leg, and a stepping recovery process of the injured person is shown Figure.1 and Figure.2. Synchronous sensing of stepping action between right foot and left foot contributes to obtain precise stepping patterns.

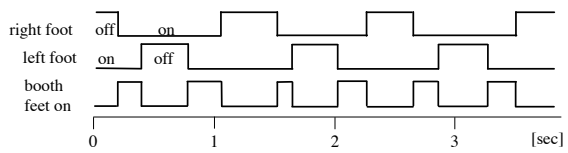

Figure.1. Stepping time diagram for the injured person.

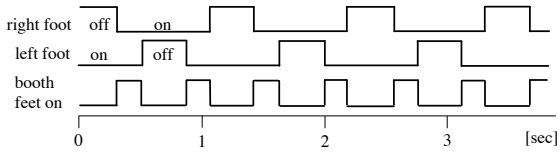

Figure.2. Stepping time diagram of 3rd experiment for the injured person.

References

1. J. Han, B. Bhanu, Individual Recognition Using Gait Energy Image, Trans. on Pattern Analysis and Machine Intelligence, Vol. 28, No.2, pp. 316-322 (2006).
2. Y. Makihara, R. Sagawa, Y. Mukaigawa, T. Echigo, Y. Yagi, Gait Recognition Using a View Transformation Model in the Frequency Domain, Proc. of the 9th European Conf. on Computer Vision, Graz, Austria, pp. 151-163 (2006).
3. K. Bashir, T. Xiang, S. Gong, Gait recognition without subject cooperation, Pattern Recognition Letters, Vol.31, No. 13, pp.2052-2060 (2010).
4. T. H. W. Lam, K. H. Cheung, J. N. K. Liu, Gait flow image: A silhouette-based gait representation for human identification , Pattern Recognition, Vol.44, pp.973-987 (2011).
5. T. Kobatyashi, Y. Miyake, Y. Wada, M. Matsubara, Kinematic Analysis System of Walking by Acceleration Sensor, Trans. Inst. Auto. Contl. Japan, Vol.42, No.5(2006).
6. J. Manyjarvi, M. Lindholm, E.Vildjounaite, S. Makela, H.Alisto, Identifying Users of Portable Devices from Gait Pattern with Accelerometers, ICAPSSP'05, March (2005).

[1]Graduate School of Science and Engineering, Kagoshima University, 890-0065, Kagoshima, Japan

Water and Environment Technology Conference 2017 (WET2017),
July 22-23, 2017, Sapporo, Japan

Synthesis, Environmental Monitoring and Risk Evaluation of Etofenprox-Ester.

Sayoko OBA[1], Fumi HASHIMOTO[1], Hirokazu TAKANASHI[1], Tsunenori NAKAJIMA[1],
Akira OHKI[1], Takehiko UEDA[1], Jun-ichi KADOKAWA[1], Hidenori ISHIKAWA[2]
and Nobukazu MIYAMOTO[2]

Abstract

Etofenprox applied to a paddy field diffuses into river water and undergoes various reactions such as hydrolysis or photolysis, resulting in formation of an etofenprox-ester, 2-(4-ethoxyphenyl)-2-methylpropyl 3-phenoxybenzoate. Since the half-life time of etofenprox is relatively long (17.5 days), the ester is less likely to be detected at high concentrations in the water environments. In this study, the concentrations of etofenprox and the ester in actual river waters were determined in order to see whether a transformation product of a pesticide is determined at lower concentration than that of its parent (intact) pesticide which has a long half-life time. The synthesis of the ester was also conducted because it was not available in the market (Figure 1 and 2). Contrary to our expectations, etofenprox and the ester were detected at high concentrations. Therefore, the acute immobilization tests with *Chironomus yoshimatsui* and *Daphnia magna* were performed to determine the acute effect concentration (AECd) of them. Fortunately the ecotoxicity risk of the ester was negligible. However, its concentration was approximately at the same level as the registration withholding limits of etofenprox (Figure 3). Consequently, monitoring concentrations of a transformation product and its parent pesticide which has a long half-life time are important to assess the ecotoxicity risk of them (Figure 4).

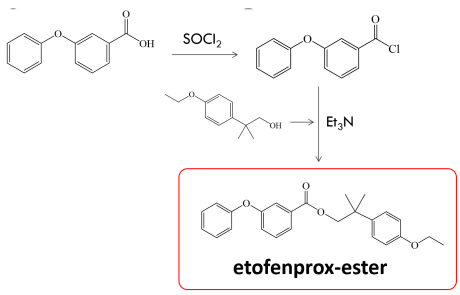

Figure 1. Synthesis of etofenprox-ester

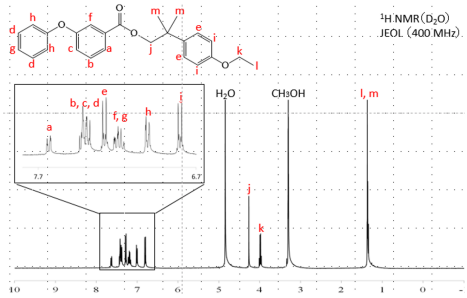

Figure 2. [1]H-NMR spectrum of etofenprox-ester

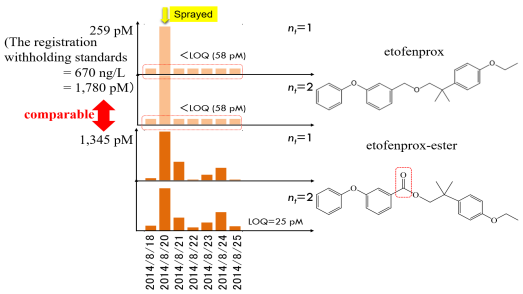

Figure 3. The concentrations of etofenprox-ester

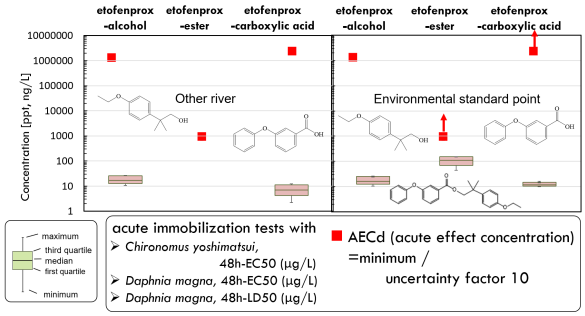

Figure 4. Risk evaluation of etofenprox PTPWs

[1] Graduate School of Science and Engineering, Kagoshima University, Kagoshima 890-0065 Japan

[2] Institute of Environmental Ecology, IDEA Consultants, Inc., Shizuoka 421-0212, Japan

The 5th Switzerland-Japan Workshop on Biomechanics 2017,
September 14-17, 2017, Zermatt, Switzerland

Dynamic characteristic changing of the external ear canal wall with an increase in neonatal chronological age

Nattikan Kanka[1], Michio Murakoshi[1], Shinji Hamanishi[2], Hiroshi Wada[3]

Abstract

A sweep frequency impedance (SFI) meter, which evaluates the dynamic behavior of the middle ear, allows the diagnosis of middle ear dysfunctions in adults and children. Recently, we have applied this method to neonates and found that the SFI data is affected by the oscillatory behavior of the external ear canal wall, rendering the diagnosis in this period of life difficult. In this study, SFI tests were regularly performed in two healthy neonates for several months, who were a full-term baby with normal perinatal history and passed the automated auditory brainstem response test. An attempt was made to clarify how long the external ear canal wall impacts on the SFI data. The measurement results suggest that the rigidity of the external ear canal wall increases with chronological age, resulting in an increase and decrease in the first variation of frequency in the sound pressure level (SPL) curve and the changes in SPL, respectively. Additionally, the oscillatory behavior of the external ear canal wall tends to be disappeared by such months of age.

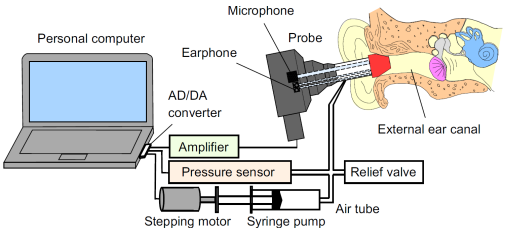

Figure 1. A schema of the SFI meter.

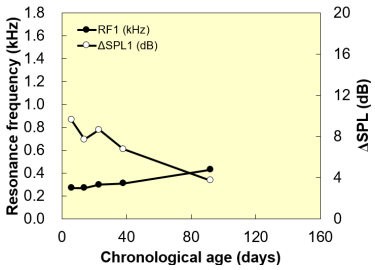

Figure 2. Chronological changes of the external ear, RF_1 and ΔSPL_1, derived from a healthy neonates.

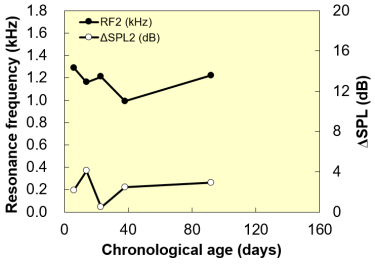

Figure 3. Chronological changes of the middle ear, RF_2 and ΔSPL_2, derived from a healthy neonates.

References

1. Morton CC and Nance WE. Newborn hearing screening –a silent revolution. N Engl J Med, 354: 2151-2164, 2006.
2. Wada H and Kobayashi T. Dynamic behavior of middle ear: Theoretical study corresponding to measurement results obtained by a newly developed measuring apparatus. J Acoust Soc Am 87 (1): 237–245, 1990.
3. Murakoshi M, Yoshida N, Sugaya M, Ogawa Y, Hamanishi S, Kiyokawa H, Kakuta R, Yamada M, Takahashi R, Tanigawara S, Matsutani S, Kobayashi T, Wada H. Dynamic characteristics of the middle ear in neonates. Int J Pediatr Otorhinolaryngol 77: 504-512, 2013.

[1] Department of Mechanical Engineering, Kagoshima University, Japan;
[2] Department of Mechanical Engineering, Sendai National College of Technology, Japan;
[3] Department of Intelligent Information Systems, Tohoku Bunka Gakuen University, Japan

Water and Environment Technology Conference 2017 (WET2017),
July 22-23, 2017, Sapporo, Japan

A Method for Monitoring Pesticide Transformation Products in Water environments (PTPWs) without their Authentic Standards

Fumi HASHIMOTO[1], Hirokazu TAKANASHI[1], Tsunenori NAKAJIMA[1], Akira OHKI[1], Takehiko UEDA[1], Jun-ichi KADOKAWA[1], Nobukazu MIYAMOTO[2], Hidenori ISHIKAWA[2]

Abstract

Pesticides are ubiquitous contaminants in water environments, so many researchers have reported their concentrations in surface waters. As well as the pesticides, Pesticide Transformation Products in Water environments (PTPWs) can be detected in the surface waters. In order to detect the PTPWs, authentic standards are needed. But the number of commercially available standards has been still limited. Thus in this study, a technique to detect the PTPWs without any of authentic standards was developed by coupling a LC-MS/MS with a high resolution LC-MS. A neonicotinoid pesticide imidacloprid was used as a model compound. Five purchasable PTPWs were detected in the irradiated aqueous solutions of imidacloprid by the analysis with the high resolution LC-MS, being acquired their retention times and m/z values. The product ion scan of the solution was conducted with the LC-MS/MS using the same chromatographic conditions, which resulted in the detection of five chromatographic peaks whose retention times are almost identical with those in the LC-MS analysis. Given this fact, SRM conditions were developed for each of these five compounds using the irradiated samples (Table 1). The developed conditions were verified by using the authentic standards, which indicates that the developed method in this study was shown to be effective (Figure 1).

Table 1. SRM conditions for imidacloprid and its PTPWs

Chemical name	CAS RN	Structure	Molecular formula / Adduct ion	Precursor ion *m/z* / RF lens [V]	Target ion *m/z* / CE [V]	Qualifier ion *m/z* / CE [V]
imidacloprid	138261-41-3	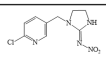	$C_9H_{10}ClN_5O_2$ / $[M+H]^+$	256 / 40	175 / 20	209 / 18
5-(aminomethyl)-2-chloropyridine	97004-04-1		$C_6H_7ClN_2$ / $[M+H]^+$	143 / 50	78 / 28	107 / 22
1-((6-chloropyridin-3-yl)methyl)imidazolidine-2-imine	127202-53-3 (115970-17-7)	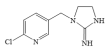	$C_9H_{11}ClN_4$ / $[M+H]^+$	211 / 60	126 / 26	99 / 40
6-chloronicotinaldehyde	23100-12-1		C_6H_4ClNO / $[M+H]^+$	142 / 80	78 / 23	106 / 18
N-(1-((6-chloropyridin-3-yl)methyl)-1,3-dihydro-2*H*-imidazol-2-ylidene)nitramide	115086-54-9	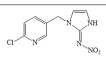	$C_9H_8ClN_5O_2$ / $[M+H]^+$	254 / 40	171 / 18	236 / 10
1-((6-chloropyridin-3-yl)methyl)imidazolidine-2-one	120868-66-8	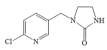	$C_9H_{10}ClN_3O$ / $[M+H]^+$	212 / 60	128 / 21	99 / 21
6-chloronicotinic acid	5326-23-8		$C_6H_4ClNO_2$ / $[M+H]^+$	158 / 28	122 / 19	78 / 23

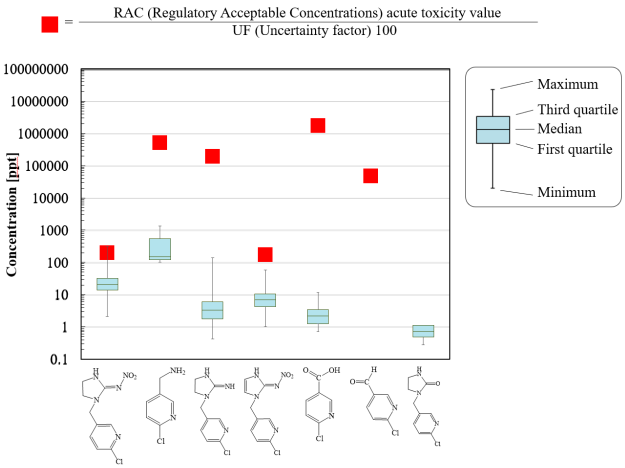

Figure 1. PTPW concentrations in the river water samples and their risk assessments

[1] Graduate School of Science and Engineering, Kagoshima University, Kagoshima 890-0065 Japan

[2] Institute of Environmental Ecology, IDEA Consultants, Inc., Shizuoka 421-0212, Japan

Nonlinear Theory and Its Applications (NOLTA) Symposium 2017,
December 4-7, 2017, Cancun, Mexico

Global Solution to Nonholonomic System with Stochastic Feedbacks Based on Non-Smooth Stochastic Lyapunov Function

Taiga Uto[1] and Yûki Nishimura[1]

Abstract

Nonholonomic systems are mechanical systems with constraints on their velocity that are not derivable from position constraints [1]. Many control systems such as cars, underwater vehicles, snake robots, and space robots are included in a class of nonholonomic systems. Hence, control problems of nonholonomic systems are important for the basic development of control engineering. However, controlling nonholonomic systems are difficult because many of them have no continuous state-feedback stabilizer [2]. Therefore, discontinuous state-feedback laws [3] or time varying state-feedback laws [4] are considered, while the designs of them are generally complicated.

Recently, the effective use of stabilization by noise is proposed for deriving a simple approach to design stabilizers for nonholonomic systems [5]. This strategy provides state-feedback laws with Gaussian white noises such that the states of the target system converges to the origin with probability one. Because disturbance terms exist, the resulting stochastic systems are represented by stochastic differential equations. The stability of the systems are analyzed via stochastic Lyapunov theory. The characteristic feature of the analysis is to deal with the systems like time-independent systems, while they are, in fact, time-varying.

Using the above strategy of stabilization by noise, we tried to stabilize a chained system by state-feedback laws with a one-dimensional Wiener process [6]. This provides stochastic control laws simpler than ones in [5] and [7]. While we designed a non-smooth stochastic Lyapunov function (SLF) for ensuring the stabilization, the proof is under construction due to the lacks of ensuring global solutions to the stochastic differential equation and analyzing the behavior of the states in the region that the SLF is non-smooth. In this paper, we show the existence of a global solution to the closed-loop system.

References

1. A. Bloch, J.E. Marsden and D.V. Zenkov, *Nonholonomic Dynamics,* pp. 1-2, 2005.
2. R.W. Brockett, Asymptotic stability and feedback stabilization, *Differential Geometric Control Theory*, pp. 181-193, 1983.
3. A. Astolfi, Discontinuous control of nonholonomic systems, *Systems & Control Letters*, Vol. 27, No. 1, pp. 37-45, 1996.
4. O.J. Sordalen and O. Egeland, Exponential stabilization of nonholonomic chained systems, *IEEE Transactions of. Automatic Control*, Vol. 40, No. 1, pp. 35-49, 1995.
5. Y.Nishimura, Stabilization by artificial Wiener processes, *IEEE Transactions of Automatic Control*, Vol. 61, No. 11, pp. 3574-3579, 2016.
6. T. Uto and Y. Nishimura, Stabilization of Nonholonomic Systems by One-Dimensional Artificial Wiener Processes, *Proceedings of SICE Annual Conference 2016*, 2016.
7. Y. Nishimura, Stabilization of Brockett integrator using Sussmann-type artificial Wiener processes, *Proceedings of 52nd IEEE Conference on Decision and Control*, 2013.

[1] Graduate School of Science and Engineering, Kagoshima University, 890-0065, Kagoshima, Japan

2017 Progress In Electromagnetics Research Symposium, May 22-25, 2017, St. Petersburg, Russia

On-chip grounded CPW line model with anomalous skin effect in THz band

Hideshi Kakiuchi[1], Yuta Sakiyama[1], Kenjiro Nishikawa[1]

Abstract

This paper proposed and analyzed a new grounded coplanar waveguide (CPW) line model with anomalous skin effect for THz integrated circuits. The proposed CPW line model employs a donut-style multilayer conductor structure. The electromagnetic (EM) simulation of the proposed 50-Ω CPW line model results in the proportion to the frequency to powers of 0.5, 0.6, and 0.67 at 0.1–0.6 THz, 0.7–1.3 THz, and 1.4–2.0 THz, respectively. These results indicate the proposed CPW line model provides more accurate characteristics caused by anomalous skin effect on EM simulation.

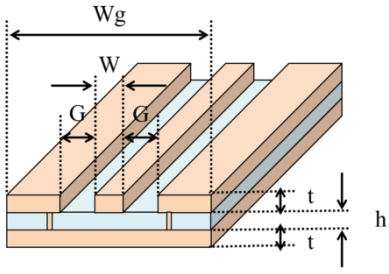

Fig1. EM simulation model of on-chip coplanar waveguide (W=2μm, G=1μm, Wg=60μm, t=1μm, h=1μm)

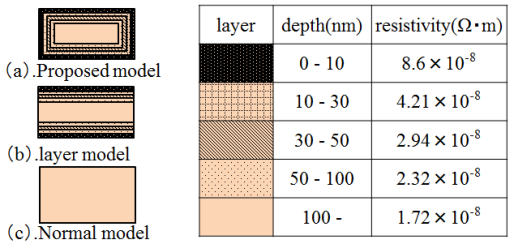

layer	depth(nm)	resistivity(Ω·m)
	0 - 10	8.6×10^{-8}
	10 - 30	4.21×10^{-8}
	30 - 50	2.94×10^{-8}
	50 - 100	2.32×10^{-8}
	100 -	1.72×10^{-8}

Fig2. Conductor model

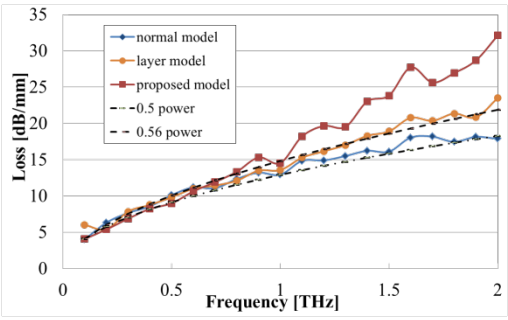

Fig3. Losses of CPW models

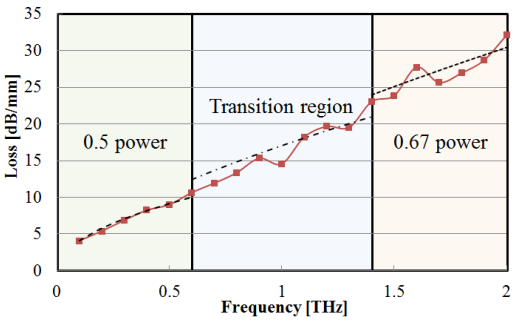

Fig4. Losses of proposed CPW conductor model

REFERENCES

[1] 2013 IEEE MTT-S IMS Workshop, WMD: Technologies for THz Integrated System. Seattle WA, June 2013.
[2] T. Hayashi,A. Sanada, and S.Nagai“Measurements on the Anomalous Skin Effect of Metal at Room Temperature in 1 THz Band” IEICE Technical Report, vol.113, no.307, MW2013-139, pp.47-50, Nov. 2013 (in Japanese).
[3] Reza Sarvari, “Impact of Size Effects and Anomalous Skin Effect on Metallic Wires as GSI Interconnects,” Ph.D. dissertation, School of Electrical and Computer Engineering, Georgia Tech., Atlanta, GA, USA, 2008.
[4] G. E. H. Reuter and E. H. Sondheimer, “Theory of the Anomalous Skin Effect in Metals,” Nature, vol.161, no.4089, pp.394-395, March 1948.
[5] Frank Schnieder,Thorsten Tischler, and Wolfgang Heinrich, ”Modeling Dispersion and Radiation Characteristics of Conductor-Backed CPW With Finite Ground Width”, IEEE Trans. on Microwave Theory Tech., vol.51, no.1, Jan. 2003.
[6] A. Tsuchiya and H. Onodera, “Gradient Resistivity Method for Numerical Evalation of Anomalous Skin Effect,” Signal Propagation on Interconnects(SPI), pp.139-142, May 2011.
[7] T. Hayashi and A. Sanada,“Measurement on the Anomalous Skin Effect of Metal at Room Temperature in 1 THz Band,” IEICE General Conference, pp.64, Mar. 2015 (in Japanese).

[1]Dept. of Electrical and Electronics Engineering, Kagoshima University, Japan

2017 IEEE MTT-S International Microwave Symposium, June 4-9, 2017, Hawaii

Design of Concurrent Dual-Band Rectifier with Harmonic Signal Control

Koshi Hamano[1], Ryuya Tanaka[1], Satoshi Yoshida[1], Akihira Miyachi[2],
Kenjiro Nishikawa[1], and Shigeo Kawasaki[2]

Abstract

This paper proposes and demonstrates a concurrent 2.45GHz/5.8GHz rectifier. The proposed concurrent dual-band rectifier drastically improves its RF-DC conversion efficiency with a harmonic signal control technique. The proposed rectifier employs two key designs. A microstrip spurline notch filter in the output section realizes high RF-DC conversion efficiencies at the dual bands. The quarter-wave length open stub of the 8.25 GHz connected at diode cathode effectively terminates the harmonic signal generated by mixing the input signals. The proposed configuration provides the high RF-DC conversion efficiency even when two-tone signals input the rectifier. The fabricated the dual-band rectifier achieves the RF-DC conversion efficiencies of 64.8 %, 62.2 %, and 67.9 % at 2.45 GHz, 5.8 GHz, and their two-tone input signals, respectively.

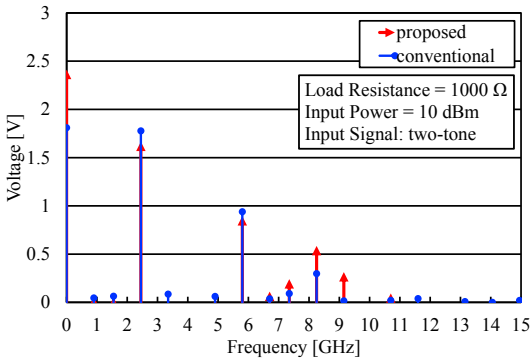

Fig. 1. Simulated frequency spectrum of voltage at diode cathode.

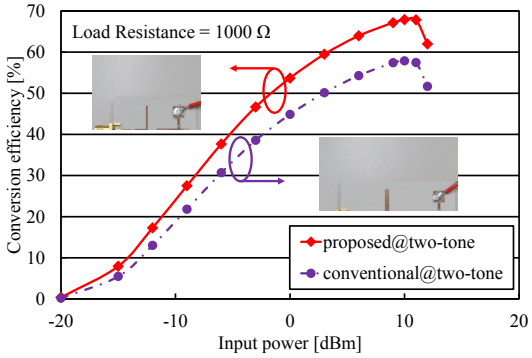

Fig. 2. Compared the proposed rectifier with the harmonic signal control to the conventional rectifier without the harmonic signal control.

REFERENCES

[1] H. Sun, Y.-X. Guo, M. He, Z. Zhong, "A Dual-Band Rectenna Using Broadband Yagi Antenna Array for Ambient RF Power Harvesting," IEEE Antennas and Wireless Propagation Lett., Vol. 12, pp. 918-921, 2013.

[2] T. Takhedmit, L. Cirio, Z. Saddi, J. D. Lan Sun Luk, O. Picon, "A novel dual-frequency rectifier based on a 180° hybrid junction for RF energy harvesting," 2013 7th European Conference on Antennas and Propagation, pp. 2472-2475, April 2013.

[3] K. Niotaki, S. Kim, S. Jeong, A. Collado, A. Georgiadis, M. M. Tentzeris, "A Compact Dual-Band Rectenna Using Slot-Loaded Dual Band Folded Dipole Antenna," IEEE Antenna and Wireless Propagation Lett., Vol. 12, pp. 1634-1637, 2013.

[4] R. Bergès, L. Fadel, L. Oyhenart, V. Vigneras, T. Taris, "A dual Band 915MHz/2.44GHz RF Energy Harvester," 2015 IEEE European Microwave Conference, pp. 307-310, Sept. 2015.

[5] J. Heikkinen, M. Kivikoski, "A Novel Dual-Frequency Circularly Polarized Rectenna," IEEE Antennas and Wireless Propagation Letters, Vol. 2, pp. 330-333, 2003.

[6] X.-B. Huang, J.-J. Wang, W.-Y. Wu, M.-X. Liu, "A dual-band rectifier for low-power Wireless Power Transmission system," Asia-Pacific Microwave Conference, pp. 1-3, Dec. 2015.

[7] D. Wang, R. Negra, "Design of a dual-band rectifier for wireless power transmission," 2013 IEEE Wireless Power Transfer, pp.127-130, Perugia, Italy, May 2013.

[8] J. A Hagerty, F. B. Helmbrecht, W. H. McCalpin, R. Zane, Z. B. Popovic, "Recycling Ambient Microwave Energy with Broad-Band Rectenna Arrays," IEEE Trans. on Microwave Theory and Techniques, Vol. 52, No. 5, pp. 1548-1553, May 2003.

[9] K. Hamano, R. Tanaka, S. Yoshida, A. Miyachi, K. Nishikawa and S. Kawasaki, "Design of Dual-Band Rectifier Using Microstrip Spurline Notch Filter," 2016 IEEE International Symposium on Radio-Frequency integration, pp.1-3, Taipei, Taiwan, Aug. 2016.

[1]Dept. of Electrical and Electronics Engineering, Kagoshima University, Japan
[2]Institute of Space and Astronautical Science, Japan Aerospace Exploration Agency, Japan

International Association for Shell and Spatial Structures (IASS) Symposium 2017,
September 25–28, 2017, Hamburg, Germany

Geometrically Nonlinear Analysis of Three Dimensional Structure Model by Finite Element Technique with Coordinates Assumption

Akinori HONDA[1], Yohei YOKOSUKA[1], Toshio HONMA[1]

Abstract

This paper describes effectiveness and significance of the geometrically nonlinear analysis using the finite element technique that adopt our expanded three-dimensional (3D) element. The geometrically nonlinear analysis of a 3D structure model came to be executed comparatively easily by recent advancement of the computer performance. However, the development of an efficient finite element is needed as 3D element. In this paper, we present the formulation of 3D element with coordinates assumption for the geometrically nonlinear analysis. An unknown variable of this element is a coordinate value of global coordinate system after the deformation on the structure model. Therefore, when the whole stiffness matrix of the structure model is built, this element doesn't need coordinate transformation at all. The finite element technique with coordinates assumption is developed for the tension structure analysis, and the effectiveness is confirmed [1,2]. Analysis model is a circular arch model. Numerical results are compared by using 3D element with the coordinates assumption and the conventional beam element with displacement assumption. Finally, we denote an example of bucking load maximization using the sensitivity analysis as the structural optimization [3].

The figures below are an analysis model and a numerical example for the circular arch of uniform section with concentrated load. It is shown that the numerical result of both elements is corresponding according to decrease of the sectional area.

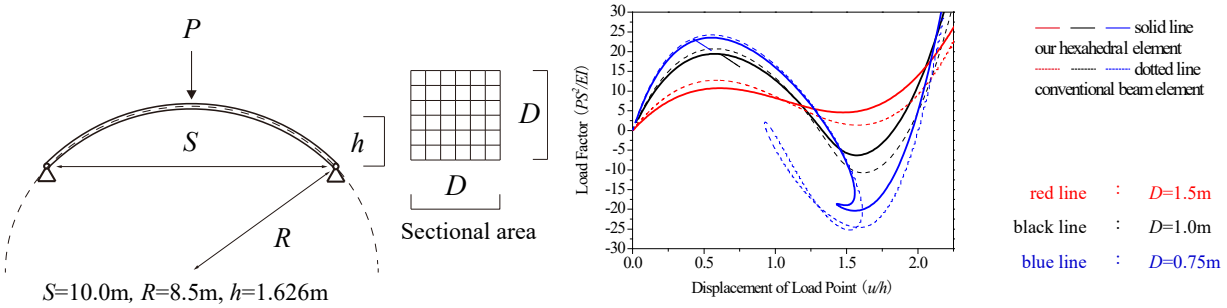

Analysis model Numerical results

Figure A numerical example for the circular arch of uniform section with concentrated load

References

1. T. Honma and N. Ataka : Geometrically Nonlinear Structural Analysis by FEM Using the Coordinate Value on a Deformed Body, information, 7(5), 569-583, 2004
2. R. Kurogi and T. Honma : Cutting Pattern Analysis with Form Finding for Pneumatic Membrane Structure and Curved Surface Form Confirmation Using Miniature Model, Proceedings of the First Conference Transformables, 423-428, 2013
3. F. Fujii and S. Shibata and T. Honma : An Effective Buckling Load Sensitivity in Shape Optimization of Nonlinear Plane Structures, 6th China-Japan-Korea Joint Symposium on Optimization of Structural and Mechanical Systems CD-ROM proceedings, J88, 2010

[1] Department of architecture & Architectural Engineering, Kagoshima Univ. 890-0065, Kagoshima, Japan

International Association for Shell and Spatial Structures (IASS) Symposium 2017,
September 25–28, 2017, Hamburg, Germany

Structural Optimization for Hybrid Structure with Cable and Strut Member: Analysis Using Finite Element Technique with Coordinates Assumption

Shingo KOMIKADO[1], Yohei YOKOSUKA[1], Toshio HONMA[1]

Abstract

In general, the hybrid structures with cable and strut member is constituted with unstable and isolated compression members. Our proposal structural model has the characteristic of tensegrity structures and cable-dome structures, and is a system with simple constructability to stabilize by only tension introduction into the cable members [1]. The structural optimization can be commonly applied to the architectural design as a design process in recent year. The form-finding methods for the hybrid structure that constitutes the self-equilibrated state with cable and strut member has a lot of researches. However, there are relatively few combined researches of the structural optimization and the form-finding analysis for hybrid structures. It is suggested that computational cost is large in this problem. Therefore, an efficient numerical analysis procedure is demanded to the structural optimization technique of this structural model.

FEM using the coordinate value on a deformed body [2] is one of the efficient form-finding analysis for cable and membrane structures. In order to apply this analysis to the hybrid structure with cable and strut member, we formulated the model with constraint conditions of specified length of compression members. The self-equilibrated state can be found by using this method as shown in figure.1.b-d. The standard genetic algorithm (SGA) is applied to the structural optimization. The design variable is length of compression members, and optimization problems are minimization of the total strain energy or the maximum displacement. In this paper, we confirm solution forms and solution spaces which are given by different objective functions.

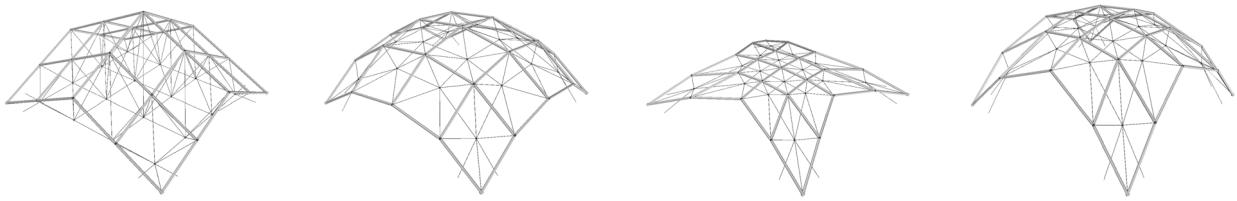

a. Initial form b. Form-0 c. Form-1 d. Form-2

Figure.1 Structural form of hybrid structure constituting self-equilibrated state with cable and strut

References

1. S.Komikado, Y.Yokosuka, T.Honma. Form-finding Analysis for Stabilized and Stiffened Structural System Using Tension Members (IASS) Symposium2016,ID1359,pp1-10,2016.
2. R. Kurogi and T. Honma. Cutting Pattern Analysis with Form Finding for Pneumatic Membrane Structure and Curved Surface Form Confirmation using Miniature Model, Proceeding of the First Conference Transformable 2013, EDITORIAL STARBOOKS, 2013.

[1] Department of architecture & Architectural Engineering, Kagoshima Univ. 890-0065, Kagoshima, Japan

8th Taiwan-Japan Bilateral Workshop
September 3-6th Tainan, Taiwan

Preparation of sugar chain-immobilized fluorescent carbon nanoparticles

Yurina Ata, Yoshiaki Manabe, Hiroyuki Shinchi, Masahiro Wakao, Yasuo Suda*

Abstruct

Sugar chains play important roles in various biological events including cell-cell recognition, cell differentiation, proliferation, and pathogen infection. Since the functional analysis of sugar chain allows us to understand their biofunction, various analytical tools using sugar chain-immobilized nanodevices such as sugar chip and sugar chain-immobilized nanoparticles have been developed to date. In our group, sugar chain-immobilized fluorescent nanoparticles (SFNPs) have been developed as fluorescent probes for sugar chain-protein interaction analysis and cell imaging.[1,2] However, the core components of the SFNPs contain toxic/carcinogenic heavy metal ion such as cadmium and indium. In this study, for expanding versatility and reducing environmental burdens of SFNPs, we focused on fluorescent carbon nanoparticles (FCNPs) prepared from naturally abundant carbon materials, and addressed preparation of sugar chain-immobilized fluorescent carbon nanoparticles (SFCNPs).

Preparation of SFCNPs is shown in Figure 1. FCNPs were prepared from L-arginine according to the method previously reported.[3] L-Arginine was carbonized by heating at 400 °C for 2 hours. The carbonized arginine was oxidized with nitric acid under reflux conditions. Occurring carboxylic acid group of FCNPs was condensed with azide linker molecule. Conjugation of sugar moiety onto FCNPs was carried out by copper-free click reaction. Sugar moieties on SFCNPs were quantified by hexose quantification using anthrone-H_2SO_4. Binding properties of SFNCPs against proteins were investigated with lectins, sugar-binding proteins, and sugar-specific aggregates were obtained.

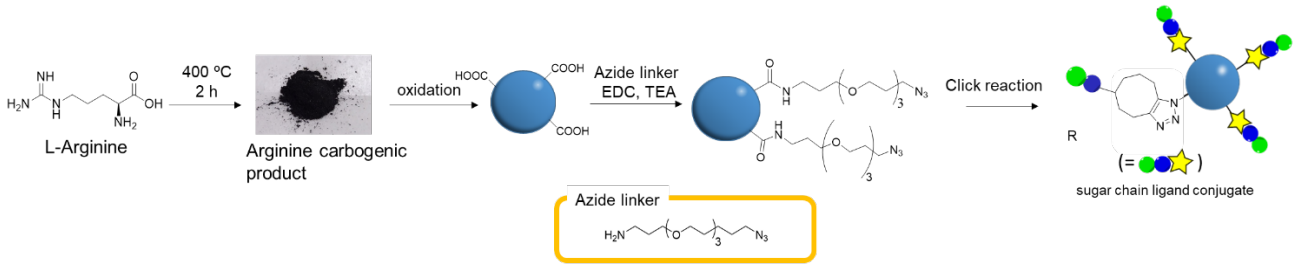

:

Figure 1. Preparation of SFCNPs.

References

1) Shinchi, H., *et al.*, *Chem. Asian. J.*, (7), 2678-2682 (2013).
2) Shinchi, H., *et al.*, *Bioconj. Chem.*, (25), 286-295 (2014).
3) Xu, Y. *et al.*, *Chem. Eur. J.*, (19), 2276-2283 (2013).

Graduate School of Science and Engineering, Kagoshima University,890-0065, kagoshima, Japan

8th Taiwan-Japan Bilateral Workshop on Nanoscience
September 3-6, 2017, Tainan, Taiwan

Synthetic study on dermatan sulfate/chondroitin sulfate hybrid tetrasaccharide structure

Takeru Oyama, Kyosuke Nishioka, Tatsuki Haranosono, Masahiro Wakao, Yasuo Suda

Dermatan sulfate (DS) and chondroitin sulfate (CS) belong to glycosaminoglycan (GAG) superfamily, and are liner sulfated polysaccharides. They are widely distributed in various tissues as components of cell membrane or extracellular matrix. DS and CS chains interact with bioactive proteins such as growth factors, cytokines, and matrix enzymes and regulate their functions. DS chain is biologically synthesized from chondroitin or CS chain by the randam and imcompleted enzymatic modification such as *C*-5 epimerase and *O*-sulfotransferase, resulting the DS/CS versatile structure. Recently, a certain DS/CS structure is considered to be important for the specific interaction with bioactive proteins, and the elucidation of structure-activity relations at the molecular level is needed for understanding their biofunctions. In this study, we addressed chemical synthesis of DS/CS hybrid tetrasaccharide structure containing DS-E (iE) and CS-E (E) units.

The synthetic strategy for iE-E tetrasaccharide structure is shown in Scheme 1. DS and CS disaccharide intermediates **1** and **2** were prepared according to the previous method,[1,2] and were transformed to DS disaccharide donor **3** and CS disaccharide acceptor **4**, respectively. Pentasaccharide precursor **5** was prepared by the glycosylation of donor **6** and acceptor **7**. iE-E tetrasaccharide structure **6** was obtained by the subsequent selective deprotection and sulfation, and the removal of the remaining protecting groups. As soon as the objective iE-E tetrasaccharide ligand conjugate **7** is obtained by the reductive amination with our original linker moiety, the molecular level analysis is performed using the Sugar Chip immobilized with conjugate 7.

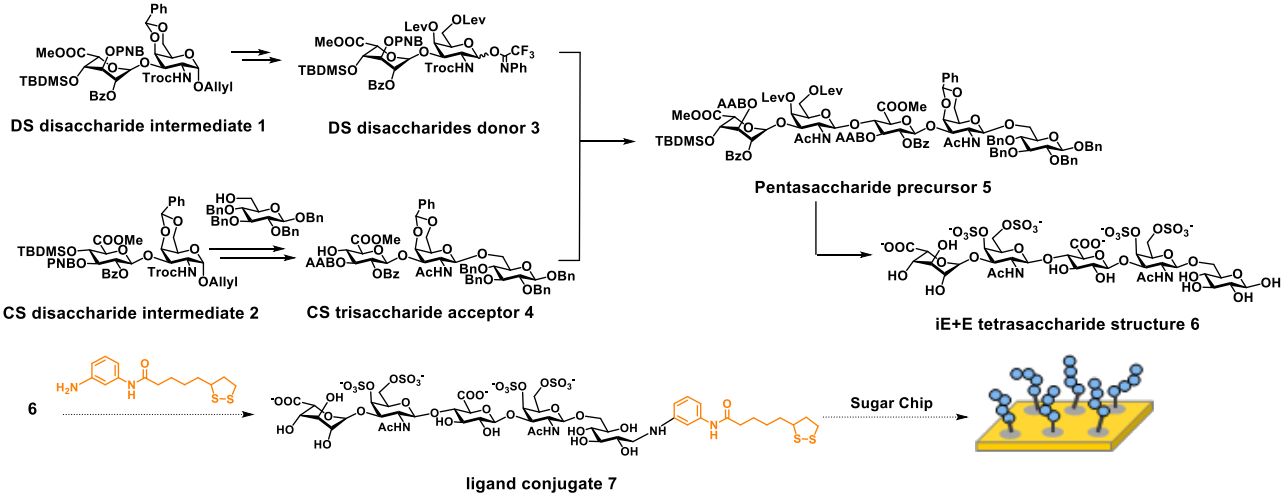

Scheme 1. Synthetic and experimental strategy for the tetrasaccharide structure containing tandem DS-E and CS-E disaccharide units.

References

1) K. Miyachi, *et al*., *Bioorg. Med. Chem. Lett*., **25**, 1552-1555 (2015).
2) Y. Kakitsubata, *et al*., *Tetrahedron Lett.*, **57**, 1154-1157 (2016).

School of Science and Engineering, Kagoshima University, 890-0065, Kagoshima, Japan

Taiwan-Japan Bilateral Workshop 2017,
Sptember 3-6, 2017, Taiwan

Development of sugar chain binding single chain variable fragment antibody to human papilloma virus (HPV)-infected cells for targeted therapy

Hayate Sawayama[1], Hiroyuki Shinchi[1], Masahiro Wakao[1], Yuji Ito[1], Yasuo Suda[1,2]

Abstract

Cervical cancer is a female specific cancer and it is considered to be caused by persistent infection of human papilloma virus (HPV). In 2012, 528,000 new cases of cervical cancer were diagnosed and 266,000 people were died worldwide. The prognosis is positive by the treatment in the early stage. However, the risk for biopsy in the diagnosis and side effects in vaccination or chemotherapy are burden for patients. Therefore, novel molecularly targeted reagent is strongly required for cervical cancer. In our group, to develop a molecularly targeted reagent, we focused on cell surface sugar chains because the expression levels and structures of cell surface sugar chains vary depending on cellular conditions including differentiation, inflammation, and concertation. Recently, we developed a cell surface sugar chain binding single chain variable fragment antibody (scFv) as a novel molecularly targeted reagent for adult T cell leukemia using our sugar chain-based nanobiotechnology and a phage display method[1]. In this study, we applied our technology to develop cell surface sugar chain binding scFvs for cervical cancer cells toward development of a novel therapeutic and diagnostic reagent.

In ca. 60-80% of patients of cervical cancer, part of HPV type-16 or -18 genes has been detected. Therefore, the genes, especially E6 and E7 in HPV-16 or -18, are biomarker for developing cervical cancer. In the present study, HeLa cells containing HPV-18 gene were used. First, HeLa cells were disrupted by homogenizer and sonication, and the cell membrane fraction was treated with Triton X-100. Then, the cell membrane proteins were separated by ultracentrifugation. The resultants proteins were treated with *N*-glycosidase F, and released *N*-linked sugar chains were captured and purified with a BlotGlyco® glycan purification kit. Purified *N*-linked sugar chains were conjugated with our original linker molecule. Obtained sugar chain ligand conjugates were analysed using MALDI-TOF/MS and several mass spectral peaks corresponding to *N*-linked sugar chain were detected. The conjugates were then separated into 4 fractions by HPLC using an ODS column. Each fraction was then immobilized on optical fiber to prepare fiber type Sugar-Chips[2]. The selectivity of the prepared chip was tested with a localized surface plasmon resonance (LPR) method and sugar chain binding proteins. Using the chip, a screening of scFv-displaying phages is now under investigation to obtain scFvs which bind to Hela cells.

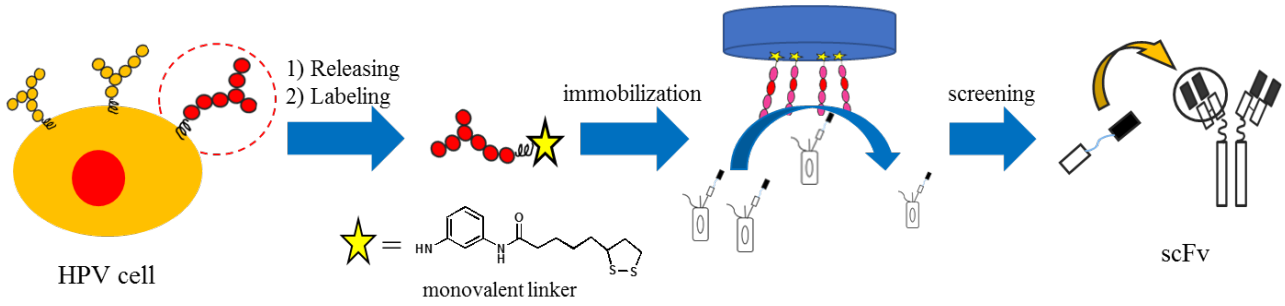

Figure. Schematic representation for developing cell surface sugar chain binding scFvs using fiber type Sugar Chip and a phage library.

Reference

[1] Muchima, K., et al. under revision. [2] Wakao, M., *et al. Anal. Chem.*, **89**, 1086-1091 (2017).

[1] Graduate School of Science and Engineering, Kagoshima University, 890-0065, Kagoshima, Japan, [2] SUDx Biotec

Synthesis and bioactivity of carbohydrate conjugates with Toll-like receptor 7 ligand 1V209

Akihito Baba[1], Hiroyuki Shinchi[1], Masahiro Wakao[1], Howard B. Cottam[2], Michael Chan[2], Tomoko Hayashi[2], Dennis A. Carson[2], Yasuo Suda[1]

Abstract

Toll-like receptor 7 (TLR7) recognizes single strand RNA (ssRNA), which is one of pathogen-associated molecular patterns (PAMPs). TLR7 is mainly located in the endosomal compartment of immune cells. Signalling through TLR7 activates the innate immune system via the adaptor protein MyD88, and shapes adaptive immune responses. Therefore, TLR7 ligands are expected to be effective reagents for anti-viral or anti-tumor therapy. Several low molecular weight TLR7 ligands, such as imiquimod and resiquimod, have been clinically approved.[1] However, their therapeutic uses has been limited due to side effects associated with cytokine release syndrome. Conjugation of the ligand with macromolecules like proteins, polysaccharides, lipids, or polymers [2-4] is a promising method to reduce or eliminate unacceptable side effects and can improve the pharmacokinetics and pharmacodynamics of the ligand. In this study, we focused on our original low molecular weight TLR7 ligand named 1V209 and carbohydrates, which are often utilized as hydrophilic tags for drug delivery system, and prepared 13 conjugates and examined their immune-stimulating activity.

The conjugation of 1V209, 2-methoxyethoxy-8-oxo-9-(4-carboxybenzyl) adenine is shown in Scheme 1. 1V209 was prepared from 2,6-dichloropurine as previously reported.[2] The conjugation with carbohydrates was done via the 9-amino group in 1V209 by a simple condensation reaction using HATU. The immune-stimulating activity of synthesized compounds was investigated on the basis of the TNF-α and interleukin-6 (IL6) production from RAW264.7 cells and mouse born marrow-derived dendritic cells (mBMDC), respectively.

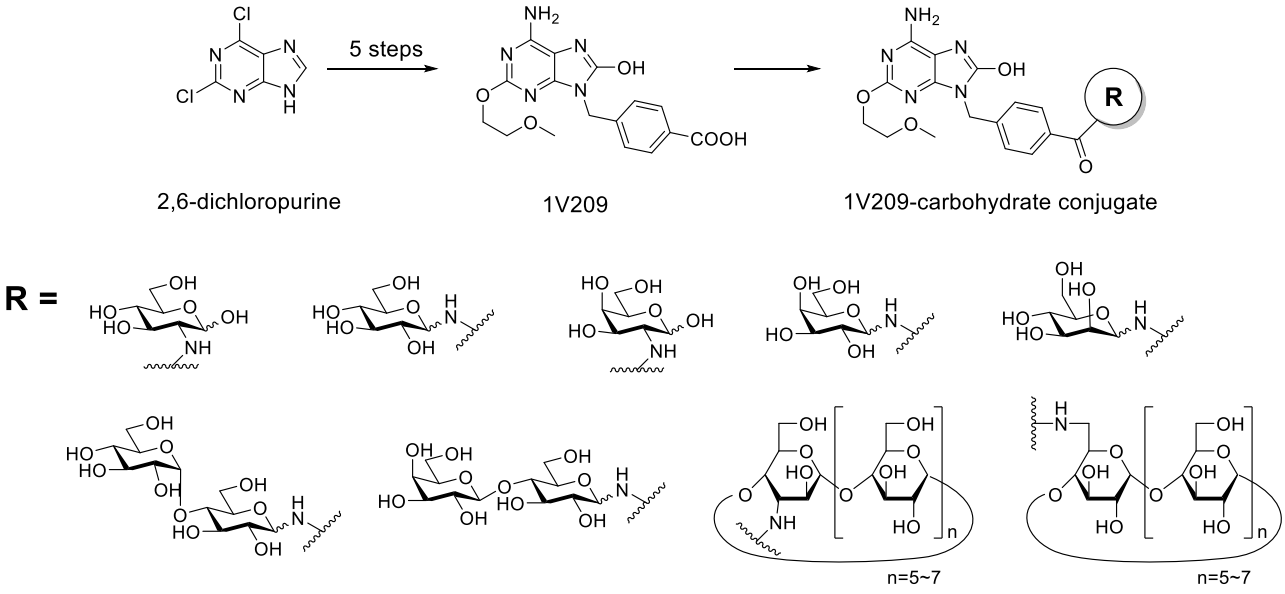

Scheme 1. Synthetic outline of TLR7 ligand-carbohydrate conjugates

References

[1] Hemmi, H., *et al., Nat. Immunol.* **3**, 196−200 (2002).
[2] Wu, C.C., *et al.*, *Proc. Natl. Acad. Sci. USA*, **104**, 3990-3995 (2007).
[3] Chan, M., *et al.*, *Bioconj. Chem.* **20**, 1194–1200 (2009).
[4] Shinchi, H., *et al.*, *Bioconj. Chem.* **26**, 1713–1723 (2015).

[1]Department of Chemistry, Biotechnology and Chemical Engineering, Kagoshima University, JAPAN
[2]Moores Cancer Center, University of California, San Diego, CA, USA

8th Taiwan-Japan Bilateral Workshop
September 3-6, 2017, Tainan, Taiwan

Development of sugar chain binding single chain variable fragment antibody toward targeted therapy for adult T-cell leukaemia

Kaname Muchima[1], Hiroyuki Shinchi[1], Masahiro Wakao[1], Yuji Ito[1], Yasuo Suda[1]

Abstract

Adult T-cell Leukaemia (ATL) is a blood cancer caused by the infection of retrovirus, human T-cell leukaemia virus type-1 (HTLV-1). Approximately 2.5-5% of HTLV-1 carriers develop ATL after an incubation period of more than 30-50 years. In Japan, HTLV-1 carriers are estimated to be approximately 1.08 million and are mainly distributed in the southwestern region of Japan including Kagoshima. Once a HTLV-1 carrier develops ATL, the prognosis is quite poor and 5-year survival rate is only ca. 10%. Specific mechanism for development of ATL has not been revealed and a standard therapy and diagnosis have not been established. In our group, to develop novel diagnostic and therapeutic drug for ATL, we focused on cell surface abnormal sugar-chain as a molecular target. Recently, three kinds of single chain variable fragment antibodies (scFvs), designated as S1TSCFR3-1, K33, and K34, were isolated from a phage library and a screening method with our Sugar Chip technology. However, the binding potencies of K33 and K34 to ATL cells are decreased in a month, indicating the low stability of the scFvs. On the other hands, S1TSCFR3-1 is very stable. In the present study, we addressed the preparation of chimera scFvs consisting of VH domain of S1TSCFR3-1 and VL domain of K33 or K34 using gene recombination.

Schematic image for the preparation of the chimera scFvs using gene recombination is shown below. pET-28b (+) DNA vector was used for a plasmid vector. A plasmid insert consisted of VH domain of S1TSCFR3-1 and VL domain of K33 or K34 were prepared using PCR. Because there is no common recognition sequence for restriction enzyme on the plasmid insert and vector, the recognition sequence for Hind III were added to the plasmid insert using TA cloning. After digestion of plasmid insert and vector using Hind III and Not I, they were ligated with ligase. The resultant plasmid was transformed into *E.coli* (BL21 (DE3) line) and several colonies were obtained. Then, the DNA sequence analysis revealed that the targeted sequence consisting of VH domain of S1TSCFR3-1 and VL domain of K33 were incorpotated into the plasmid. Preparation of the soluble scFv is now ongoing.

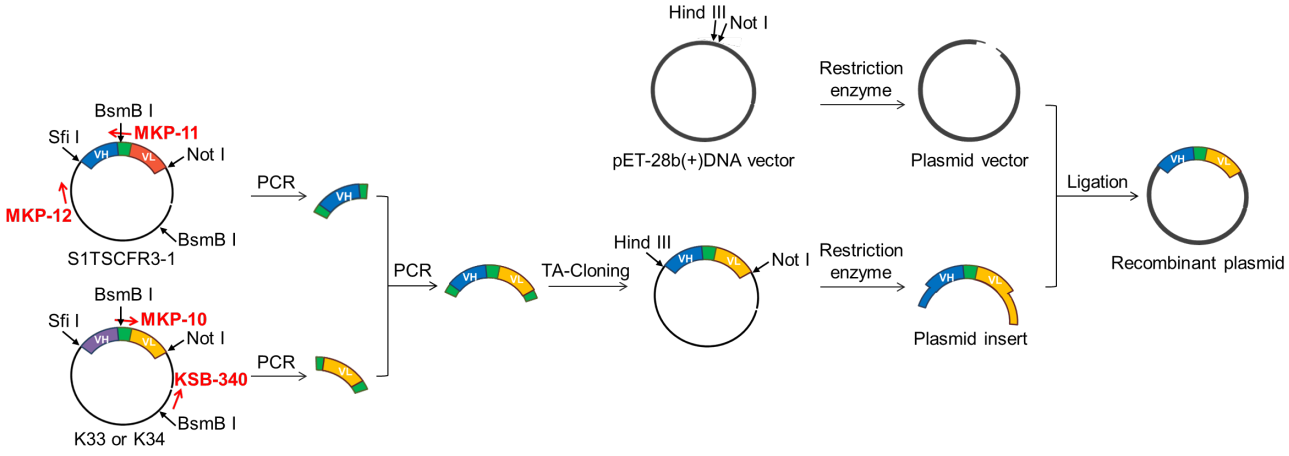

Figure. Schematic image for preparation of *O*-glycan binding scFv using gene recombination

[1] Graduate School of Science and Engineering, Kagoshima University

The 30th International Symposium on Chemical Engineering, December 1-2, 2017,
KAIST, Daejeon, Korea

Study of reactor model of fluidized catalyst bed utilizing hydrogenation of carbon dioxide

Kyosuke Daian, Takami Kai, Tsutomu Nakazato

Abstract

Fluidized catalyst bed reactors are used in many chemical processes. However, despite the fact that there are many reactions in which fluidized beds are considered to be suitable as reactors, they are currently not fully utilized. One of the reasons is that scale up and design methods are not sufficiently established. In many cases, it is hard to explain the results of chemical reactions by reactor models. Namely, the models have not been effectively utilized [1, 2]. Levenspiel [3] pointed out that the uncertainty of the bubble diameter of the fluidized bed made the design and scale-up difficult. In addition, Tsutsui [4] has emphasized the role of the direct contacting particles that are the particles in contact with a gas concentration of bubbles. In this study, the hydrogenation of carbon dioxide was performed as a model reaction. Based on the experimental results, the axial distribution of the contact efficiency and the roles of contact efficiency of direct contacting particles are studied to examine the fluidized bed model that can accurately predict the reactor performance.

The reactor was made of a glass column with an inner diameter of 45 mm and height of 1.5 m. Because a transparent heater was coated on the outer surface of the column, it is possible to observe the inner surface of the column during the bed was fluidized by reactant gases and reactions were performed. The hydrogenation of carbon dioxide was performed over the catalyst of 20 wt% Ni-La_2O_3-Pt /Al_2O_3. The content of Pt was 0.05 wt%. The carrier was the porous alumina particles. The particle diameter and particle density were 55 μm and 880 kg/m^3, respectively. The reaction was performed by changing the gas velocity, the reaction temperature and the settled bed height.

The conversion was slightly higher for the lower gas velocity at the same temperature. At the same gas velocity, the conversion increased with settled bed height. This is due to the increase in the contact time between the reaction gas and the catalyst particles. The overall reaction rate constant K_{OR} was obtained by using the experimental results. The higher settled bed height was, the lower K_{OR} became. This is considered to be that the bubble diameter is small in the bottom of the bed and the mass transfer capacitance coefficient increased due to the large interface area between the bubble and the emulsion phase.

Figs. 1 and **2** show the values of $k_{ob}a_b$ and v that correspond to the value of K_{OR} obtained in the experiments for each condition. The values of $k_{ob}a_b$ increased with decreasing settled bed height. This was caused by the bubble growth for the bed with high settled bed height.

In addition, the fraction of the direct contacting particles increased with settled bed height. At the upper part of the bed, several small bubbles gather and rise. This situation can be seen as a large bubble containing much particles in it [9]. The above tendency can be explained by considering these particles as the direct contacting particles.

Both the parameters, $k_{ob}a_b$ and v increased with gas velocity as shown in these figures. When the gas velocity increased, the number of bubbles increased, and the interface area also increased. Therefore, these parameters increased with gas velocity. In the case of this study, when the fraction of the direct contacting particles was 2–15%, the experimental results could be explained. Therefore, the role of the direct contacting particles cannot be ignored.

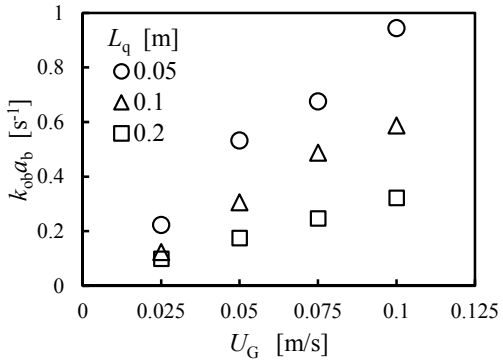

Fig. 1 Effect of gas velocity on the mass transfer capacitance coefficient

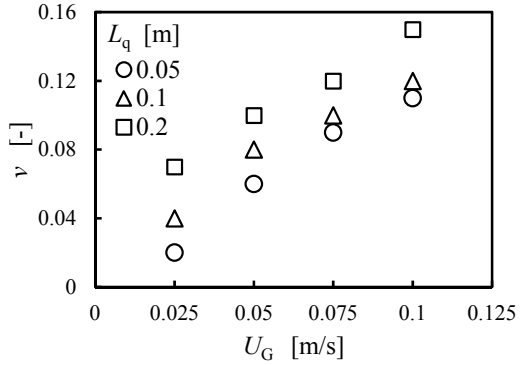

Fig. 2 Effect of gas velocity on the fraction of the direct contacting particles

Literature Cited

1) D. Newton, *et al*., *Powder Technol*. **120**, 70–75 (2002)
2) N. Mostoufi, *et al*., *Ind. Eng. Chem. Res*. **40**, 5526–5532 (2001)
3) O. Levenspiel, *Ind. Eng. Chem. Res.*, **47**, 273–277 (2008)
4) T. Tsutsui, *Kagaku Kogaku Ronbunshu*, **30**, 249–255 (2004)
9) T. Kai *et al*., *Powder Technol*., **129**, 22–29 (2003)

Department of Chemical Engineering, Kagoshima University,
Kagoshima 890-0065, Japan

The 30th International Symposium on Chemical Engineering, December 1-2, 2017,
KAIST, Daejeon, Korea

Range of particle properties affecting the defluidization caused by gas switching

Kosuke Terachi, Takami Kai, Tsutomu Nakazato

Abstract

Gas-solid fluidized beds are used in various fields such as catalytic reaction, combustion, gasification and granulation. Fluidizing gas is not usually switched in the steady state operation. However, this operation is performed to change reactant gases with an inert gas when starting up or shutting down operation. Rietema and Hoebink[1] reported that the defluidization occurred when the lower density gas was switched to the higher density gas. Kai and Takahashi[2] investigated the influence of gas properties in detail. As the result, they found that the intensity of the defluidization depends on the difference in the reciprocal route of the molecular weight of the two gases. They considered the non-equimolar counter diffusion and the bulk flow due to the pressure difference to describe this phenomenon and proposed a model based on this idea. It has been reported that simulation of non-equimolar diffusion phenomenon in an isobaric system called Graham's law can be performed and the experimental results by other researchers can be explained well[3]. The purpose of this study is to clarify the influence of particle properties on the defluidization. In addition, the methods to mitigate the influence of defluidization is proposed.

An acrylic resin tube was used for the construction of fluidized bed. The inner diameter and height were 52 mm and 1500 mm, respectively. The combination of gases was H_2/N_2, H_2/Ar, He/N_2 and He/Ar. Porous silica particles were fluidized. In the experiments, the first gas was supplied and the stable fluidization was confirmed. Then the data sampling by a pressure sensor was started. The fluidizing gas was changed to the second gas after 10 s. This procedure was repeated five times to determine the average value of the pressure change.

Based on the experimental results obtained by changing particle size and density for H_2/Ar system, the values of the three parameters in the correlation were determined. **Fig. 1** shows the relationship between particle diameter and particle density that bring η = 0.01 and η = 0.05. The difference between the particle properties when η = 0.01 and η = 0.05 was small. By assuming that defluidization does not occur when η is less than 0.01, the region is beyond the curve for η = 0.01. On the other hand, defluidization will possibly occur in the region below the curve. In addition, the intensity of defluidization increase the particle properties is far from the curve. Fig. 2 also shows the particle properties that are used for fluidized catalyst beds as region AA [4]. This figure clearly indicates that defluidiztion highly likely occur in fluidized catalyst beds.

In this study, a gradual change of gases is evaluated to avoid defluidization. A wind box was installed on the gas feed line just before the fluidized bed. The first gas and the second gas were mixed in the box and the mixture was supplied to the fluidized bed. The gas replacement time was varied by varying the volume of the wind box. The change in gas composition with time was measured by gas chromatography. The replacement time increased with increasing the box volume. **Fig. 2** shows the pressure change when gas is gradually switched from He to Ar. The induction time of defluidization increased with the replacement time, t_S. In addition, the intensity of defluidization decreased with increasing t_S. When t_S was 310 s, channeling did not occur and a good fluidization could be maintained. It was found that temporary defluidization due to non-equimolar diffusion can be prevented by the gradual gas switching.

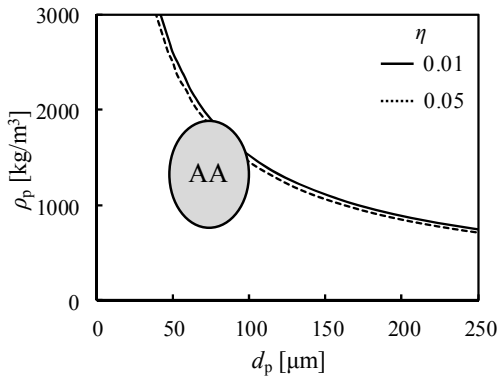

Fig. 1 Range of particle properties having possibility of defluidization by the gas switching.

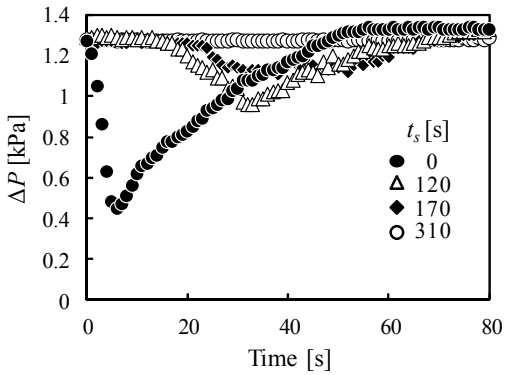

Fig. 2 Effect of the time required for substitution of fluidizing gas from He to Ar.

Literature Cited

1) Rietema, K., J. Hoebink, *Powder Technol.*, **18**, 257–265 (1977)
2) Kai, T., T. Takahashi, *AIChEJ.*, **43**, 357–362 (1997)
3) Kai, T., *Kagaku Kogaku Ronbunshu*, **43**, 271–280 (2017)
4) Kai, T. *et al.*, *Ind. Eng. Chem. Res.*, **43**, 5474-5482 (2004)

Department of Chemical Engineering, Kagoshima University, Kagoshima 890-0065, Japan

2nd International Christmas Caparica Congress on Translational Chemistry

4-7 December 2017, Caoarica, Portugal

Composite Materials from Two Kinds of Chitin Nanofibers

Koki Sato, Kazuya Yamamoto, Jun-ichi Kadokawa*
Graduate School of Science and Engineering, Kagoshima University
*kadokawa@eng.kagoshima-u.ac.jp

Abstract

Chitin is a natural polysaccharide composed of β(1→4)-linked *N*-acetyl-D-glucosamine units. Although chitin is one of the most abundant polysaccharides on the earth, it is mostly poor in processability and solubility due to strong crystalline structure by numerous hydrogen bonds. It has been well accepted that the construction of nanostructures is an efficient method for chitin materialization [1]. We have successfully prepared chitin nanofibers in two ways based on top down and bottom up approaches. We already reported by the former approach that an amidinated chitin was converted into a cationic amidinium chitin nanofibers by CO_2 gas bubbling in water [2]. On the other hand, by the latter approach, we found that self-assembled chitin nanofibers were obtained by regeneration from a chitin ion gel with 1-allyl-3-methylimidazolium bromide using methanol [3]. In this study, we performed the preparation of composite materials from the two kinds of chitin nanofibers by electrostatic interaction (Scheme 1). Anionic chitin nanofibers were first prepared by the reaction of maleic anhydride with hydroxy groups on self-assembled chitin nanofibers. For composition, the partially maleylated chitin nanofiber dispersion, which was prepared by stirring in aqueous ammonia, was then added to an amidinium chitin nanofiber aqueous dispersion and stirred. The morphology of the isolated composite sheet from binary chitin nanofibers at nano-scale was evaluated by SEM measurement.

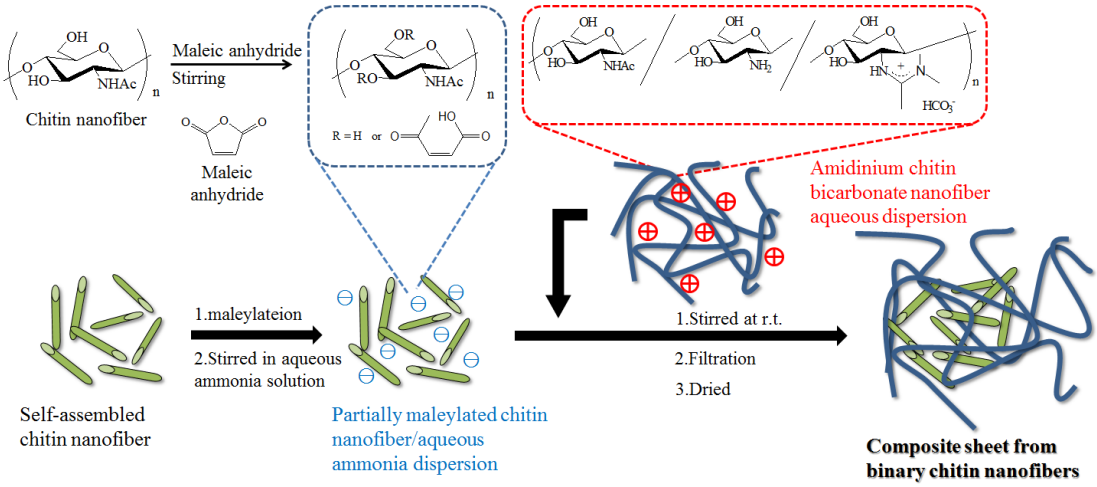

Scheme 1. Preparation of composite sheet from cationic and anionic chitin nanofibers

References

[1] S. Ifuku, Molecules 19 (2014) 18367-18380.
[2] K. Tanaka, K. Yamamoto, J. Kadokawa, Carbohydr. Res. 398 (2014) 25.
[3] J. Kadokawa, A. Takegawa, S. Mine, K. Prasad, Carbohydr. Polym. 84 (2011) 1408.

Department of Chemistry, Biotechnology, and Chemical Engineering, Graduate School of Science and Engineering, Kagoshima University, Kagoshima 890-0065, Japan

2nd International Christmas Caparica Congress on Translational Chemistry

4-7 December 2017, Caparica, Portugal

Amylose Analog Aminopolysaccharide: A New Polysaccharide Material

Takuya Nakauchida, Kazuya Yamamoto, Jun-ichi Kadokawa*

Graduate School of Science and Engineering, Kagoshima University

*kadokawa@eng.kagoshima-u.ac.

Abstruct

Natural polysaccharides exhibit specific important functions, which are profoundly affected by subtle difference in the chemical structure. Accordingly, enzymatic approach is well accepted as a powerful tool to provide well-defined polysaccharides because enzymatic reaction is progressed with highly controlled regio- and stereoarrangements. Phosphorylase is one of the enzymes, which have been used as catalysts for the synthesis of polysaccharides. This enzyme catalyzes enzymatic polymerization of α-D-glucose 1-phosphate and its analog substrates initiated from the nonreducing end of a maltooligosaccharide primer to produce some α(1→4)-linked polysaccharides [1,2]. For example, we reported that thermostable phosphorylase catalyzed enzymatic polymerization of α-D-glucosamine 1-phosphate (GlcN-1-P) as a monomer initiated from a maltotriose primer to give amylose analog aminopolysaccharide [3].

To obtain functional materials from the aminopolysaccharide, in this study, we performed its reductive amination using $NaBH_3CN$ as a reductant to obtain aggregated polysaccharide materials. The ^1H NMR spectra of the products, which were obtained using 3-5 equivs. of the reductant with the reducing end of the aminopolysaccharide, supported the progress of the reaction. The SEM images of spin-coated samples of the products observed morphology of nanoparticles. The DLS profiles of the products showed that average diameters of the nanoparticles increased with increasing the feed ratios of the reductant. Hydrogels were obtained when large equivs. of reductants were employed.

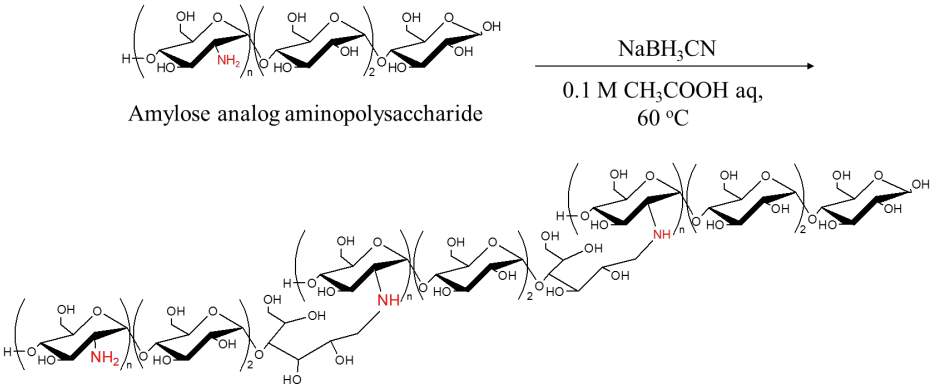

Scheme 1. Reductive amination of amylose analog aminopolysaccharide.

References

[1] G. Ziegast, B. P fannemüller, Carbohydr. Res. 160 (1987) 185
[2] S. Shoda, H. Uyama, J. Kadokawa, S. Kimura, S. Kobayashi, Chem. Rev. 116 (2016) 2307
[3] J. Kadokawa, R. Shimohigoshi, K. Yamashita, K. Yamamoto, Org. Biomol. Chem. 13 (2015) 4336

Department of Chemistry, Biotechnology, and Chemical Engineering, Graduate School of Science and Engineering, Kagoshima University, Kagoshima 890-0065, Japan

The 30th International Symposium on Chemical Engineering (ISChE 2017),

December 1-3, 2017, KAIST Daejeon, Korea

Cleaning enhancement of solid dirt on plates with water containing fine air bubbles

T. Fukatani[1], T. Goshima[1], K. Mizuta[1] and S. Nii[1]

Abstract

Cleaning requires a large amount of water and chemicals which need treatment before emission. Reducing the amount of water and chemicals is the major subject to develop greener processes. The application of fine bubbles, FB, of air to cleaning has been attracting attention because of the potential of realizing chemical free cleaning processes. The advantage of cleaning enhancement was reported by Matsuura et al. [1] and Reuter et al. [2]. Although there is an enhancement of cleaning, the quantitative evaluation is still unclear and the characteristic of fine bubbles is rarely described.

The present study focuses on measuring mass-transfer coefficient of the dirt material in various operating conditions and also to discuss the working mechanism of fine bubbles on the cleaning enhancement. The analysis of fine air bubbles in water helps to elucidate effective bubbles for the enhancement.

Benzoic acid was selected as a model solid dirt on a plate. A glass plate coated with benzoic acid was set in the duct. Water containing fine air bubbles was force to flow in the duct. The weight reduction of benzoic acid and the change of area were measured to calculate the mass-transfer coefficient of benzoic acid. Distribution of bubble diameter and the number density of bubbles in water were analyzed with a laser diffraction method.

The mass-transfer coefficient for the presence of fine air bubbles was 1.4 times greater than water without fine bubbles. Dependence of the coefficient against flow velocity was compared with the conventional mass-transfer from flat plate and it was found that the presence of FB enhanced 10 % of the dependency against flow velocity.

References

1. K. Matsuura, et al.; Separation and Purification Technology, 142, 242-250, 2015
2. F. Reuter, et al.; Ultrasonics Sonochemistry, 29, 550-562, 2016

[1] Department of Chemical Engineering, Kagoshima University, 890-0065, Kagoshima, Japan

Coalescence Enhancement of Oil Droplets in W/O Emulsions with Packed-Bed Type Coalescers

Satoru Nozawa[1*], Katsuki Kikuchi[1], Takashi Goshima[1], Kei Mizuta[1], Tatsuya Masui[2] and Susumu Nii[1]

1. Introduction

Separation of oil droplets from W/O emusion is important for both reducing environmental impact and recoverying resources. Coalescer has advantages of simplicity in the operation and no additional chemicals required. When W/O emulsions flowed through the coalescer consisting of PTFE fiber bed, oil drops would successfully coalesce and grow at the outlet of the bed. Visual observation proved that the spreading of oil film on fiber surface and flowing of oil along the fibers. The finding suggested that the importance of affinity of oil and surface of the fiber as well as narrow spacings in the fiber bed. Although capturing oil droplets in the bed is a complex phenomena, surface property of the fiber material should play an important role. Thus, for developing the perfrmance of coalescer, the present study aims to examine the effect of property of polymeric fibers or foam on the separation performance.

2. Experimental

Tetradecane is selected as an oil and 3 cm^3 of tetradecane was mixed with deionized water. The mixture was vigorously stirred with an ultrasonic homogenizer to prepare W/O emulsion. Fibers of polytetrafluoroethylene, PTFE, and polypropylene, PP, and foam of polyurethane, PU, were selected as packing material. Packed beds of these fibers and a foam were used as coalescer. **Figure 1** shows the schematic diagram of experimental apparatus. The feed was supplied to the coalescer and the pressure drop was measured with a manometer. Samples were taken from feed reservoir and effluent. The absorbance was measured to determine the separation ratio.

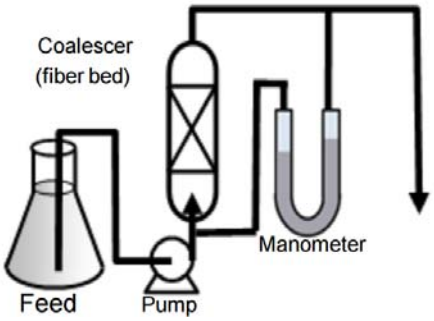

Fig.1 Experimental setup

3. Results and Discussion

Figure 2 shows a result of separation ratio and pressure drop of various polymer fiber bed. Compared to the result of PTFE as a benchmark, the material and the structure of fiber affected the performance. The difference between PP-A and PTFE reflects the effect of material because the two beds have a similar volume fraction. PP-B gave a better separation than PP-B which has a different structure of the fiber, square cross-section of the fiber. PU exhibited the maximum separation factor with much lower volume fraction. However, PU showed the highest pressure drop. The result clearly shows the effect of material properties as well as the physical spacial structure of the fiber bed.

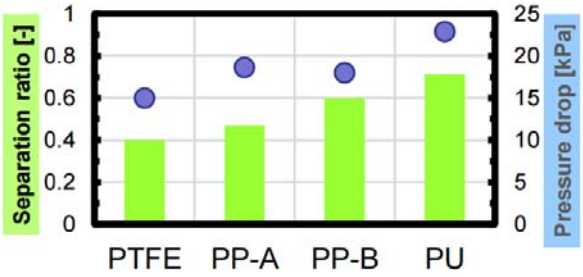

Fig.2 Effect of fiber type on separation ratio and pressure drop

1. Department of Chemical Engineering, Kagoshima University, JAPAN, 2. Morimatsu Industry Co.,Ltd,1430-8,Minobe,Motosu,Gifu 501-0413, JAPAN

The 30th International Symposium on Chemical Engineering,
December 1-2, 2017, Daejeon, South Korea.

Drying of diluted egg white droplets using a drying-aid agent in a powder-particle spouted bed

Naoya Hamahata[1], Tsutomu Nakazato[1] and Takami Kai[1]

Abstract

Currently, Kagoshima Prefecture has maintained a top three domestic market share in chicken egg production. Manufacturing egg-processed food, especially where only egg yolk is necessary and separated, is often accompanied by the discharge of a large amount of egg white. Egg white separated from the production line can be reused as it is or as a powder after being sprayed for drying, but smaller companies cannot always afford to do so because post-processing of egg white needs extra cost. Imparting various added-values to egg white is desired [1] if we want to reuse it in other way.

From the chemical engineering point of view, egg white can be rapidly dried from its droplets without a spray by using a Powder-Particle Spouted Bed (PPSB), which has been proven to be effective to simultaneous drying and chemical reaction of slurry materials [2]. Furthermore, adding drying-aid agent to the raw material can make it possible to improve drying of egg white in the bed.

In this study, drying performance of a PPSB was investigated by changing the amount of SiO_2 added to an egg white solution diluted with water by 1:1 and then subjected to pH adjustment to 6-7 by adding 0.5M-HCl. Continuous operation for 60 min was chosen as a criterion for stable operation. Our study clarified that SiO_2 addition to diluted egg white solutions can realize stable operations of a PPSB even with higher feeding rates of raw liquid material.

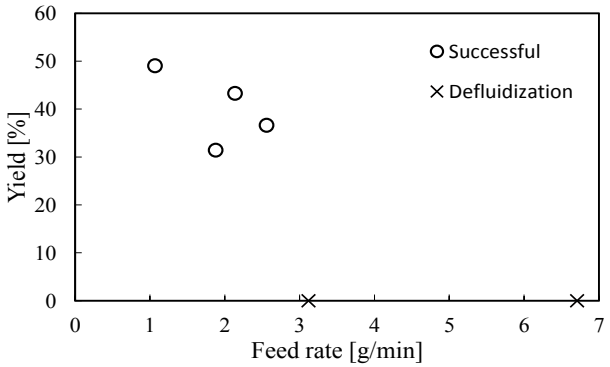

Figure 1. Relation between yield of egg white powder and feeding rate of raw liquid material (SiO_2: 0%)

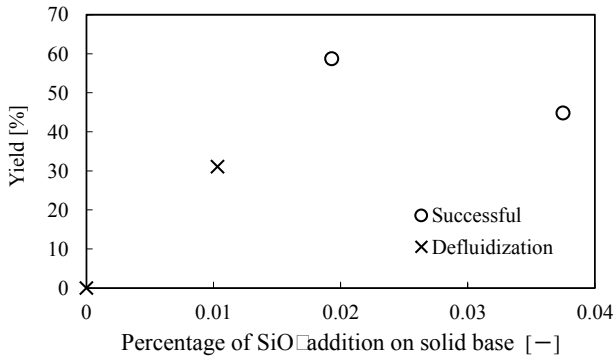

Fig. Relation between yield of egg white powder and percentage of SiO_2 addition on solid base to raw liquid material (Feeding rate: ~3.50 g/min)

References

1. Y. Mine: Effect of pH during the dry heating on the gelling properties of egg white proteins, *Food Res. Internat.*, **29**, 155-161 (1996)
2. T. Nakazato, Y. Liu, K. Sato and K. Kato: Semi-dry Process for Production of Very Fine Calcium Carbonate Powder by a Powder-Particle Spouted Bed, *J. Chem. Eng. Japan*, **35**, 409-414 (2002)

[1] Department of Chemical Engineering, Kagoshima University, 890-0065, Kagoshima, Japan

The 30th International Symposium on Chemical Engineering,
December 1-2, 2017, Daejeon, South Korea

Heat Treatment of Apatite-type Catalyst Particles Using a Fluidized Bed for Propane Oxidative Dehydrogenation

Yukinori Kumeda[1], Tsutomu Nakazato[1], Takuya Ito[1] and Takami Kai[1]

Abstract

Hydroxyapatite ($Ca_{10}(PO_4)_6(OH)_2$, HAp) has been used as an industrial material as a HPLC adsorbent, acid-base catalyst, and as an ion exchanger. Recently, HAp containing small amounts of Fe (Fe-HAp) has been reported to exhibit higher activity than normal HAp in propane oxidative dehydrogenation (PODH) [1]. Since HAp possesses high ion exchangeability, it is possible to substitute some part of Ca site with useful catalyst metals. Our recent preliminary study on the Fe-HAp catalyst found that heat treatment under a reduced atmosphere can effectively promote catalytic activity. In addition, it is expected that catalytic activity of Fe-HAp can be enhanced by drip thermal treatment in a fluidized bed; a method which was once applied to the enhancement of catalytic activity of Ni-HAp in the partial oxidation of methane [2]. In this study, we aim to develop unprecedented high activity HAp catalyst by specifying metal active species suitable for substitution to HAp and conducting fluidized bed thermal reduction treatment. HAp catalysts containing various metal species (M-HAp) as catalytically active species were prepared using a fluidized bed.

HAp catalysts containing various metal species as catalytically active species were prepared by adding the metals to either acid solution including P or base suspension including Ca with a constant molar ratio of Ca/M = 9/1 keeping a stoichiometric ratio of Ca/P to be 1.667. This study clarified that M-HAp catalysts showing higher catalytic activities so far were successfully prepared as compared with other catalysts reported in the literature. In particular, HAp catalysts with cobalt, vanadium and molybdenum incorporation showed better catalytic activity in PODH (Fig.1).

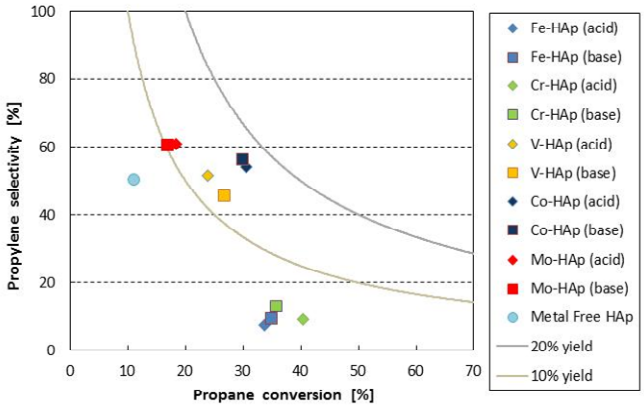

Figure 1. Propane conversion and propylene selectivity for M-HAp catalysts prepared in this study.

References

1. M. Khachani, M. Kacimi, A. Ensuque, J.-Y. Piquemal, C. Connan, F. Bozon-Verduraz and M. Ziyad: Iron-Calcium-Hydroxyapatite Catalysts : Iron Speciation and Comparative Performances in Butan-2-ol Conversion and Propane Oxidative Dehydrogenation," *Applied Catalysis A: General*, **388**, 113-123 (2010)
2. T. Nakazato, M. Kaya and T. Kai: "Drip pyrolysis in a Fluidized Bed for preparation of Nickel-Hydroxyapatite Catalyst for Partial Oxidation of Methane," Proceedings of the 10th China-Japan Symposium on Fluidization, pp.112-117, Tokyo, Japan (2010)

[1] Department of Chemical Engineering, Kagoshima University, 890-0065, Kagoshima, Japan

Taiwan-Japan Bilateral Workshop 2017 (2017 TJBW)September 3-6, 2017, Tainan, Taiwan

Preparation of soluble polysilsesquioxane containing macrocyclic structure by sol-gel reaction and metal ions capture

Daisuke Maeda,[1] Kimihiro Matsukawa,[2] Yasunari Kusaka,[3] Yoshiro Kaneko*,[1]

Abstract

Polymers containing macrocyclic structures, that can capture atoms or molecules depending on the ring size and the functional groups, are expected as metal scavengers and stationary phases for chromatographic separation. However, only a few studies regarding the preparation of such polymers containing macrocyclic structure.[1] On the other hand, silsesquioxanes (SQs) have attracted much attention in the fields of organic-inorganic hybrid materials because they are inorganic materials indicating remarkable compatibility with organic compounds such as polymers, in addition to exhibiting superior thermal, mechanical, and chemical stabilities due to siloxane (Si-O-Si) bond frameworks. However, the regularly structured soluble polySQs (PSQs) have only been obtained in limited cases.[2,3] In this study, we found that soluble PSQ containing macrocyclic structure (PSQ-MC) was successfully prepared by the hydrolytic condensation of dual-site silane coupling agent, bis{3-[3-(trimethoxysilyl)propylthio]propyl}phthalate (BTPP),[4] using HCl as a catalyst in ethyl acetate/acetone mixed solvent. In addition, we investigated the capture of metal ions using PSQ-MC.

PSQ-MC was prepared by the following procedures: Acetone solution of HCl was added to BTPP in ethyl acetate with stirring at room temperature and this solution was further stirred for 24 h. Then, the solution was heated (*ca*. 50 °C) in an open system until the solvent was completely evaporated (Scheme 1). After the product was dissolved in ethyl acetate, the solution was added to toluene. Then, the toluene-insoluble part was recovered by decantation to remove the low molecular weight components. PSQ-MC was soluble in organic solvents, such as DMSO, acetone, ethyl acetate, and chloroform. ^{1}H NMR spectrum of PSQ-MC exhibited the peaks corresponding to the side chain structure of the polymer. The weight average molecular weight of PSQ-MC estimated by GPC was *ca*. 3.8×10^4. Solid-state ^{29}Si NMR spectrum exhibited broad peaks in the T^3 and T^2 regions. Their integral ratio was *ca*. 1:1, which exhibited the presence of large amount of silanol (Si-OH) groups in the product. Because PSQ-MC was soluble polymer with high molecular weight, we assume that this PSQ is not a polymer with random structure. Conversely, ladder-like PSQs are generally known as soluble PSQ. However, since PSQ-MC contained a large amount of silanol groups, it seems that the present PSQ is not ladder-like PSQ, which has only a small amount of silanol groups. Detailed studies on its structure are now in progress.

Furthermore, we investigated the capture of Pd ions using PSQ-MC. $PdCl_2$ was dissolved in HCl aq. and this solution was added to chloroform solution of PSQ-MC. Then, this mixture was stirred for 30 min. Consequently, we visually confirmed that chloroform layer was colored. EDX pattern of the solid product obtained by drying the chloroform layer exhibited the peaks assigned to Pd. Therefore, PSQ-MC has the capability to capture Pd ions.

References

1) B. Ochiai and T. Endo et al., *J. Am. Chem. Soc.*, **130**, 10832 (2008).
2) J. F. Brown, Jr. et al., *J. Am. Chem. Soc.*, **82**, 6194 (1960).
3) Y. Kaneko et al., *Chem. Eur. J.,* **20**, 9394 (2014).; *Polymer*, **121**, 228 (2017).
4) K. Matsukawa et al., *J. Photopolym. Sci. Technol.,* **27**, 261 (2014).

[1]Graduate School of Science and Engineering, Kagoshima University, Kagoshima, Japan; [2]Materials Science and Technology, Kyoto Institute of Technology, Kyoto, Japan; [3]Sekisui Chemical Co., Ltd., Osaka, Japan

Taiwan-Japan Bilateral Workshop 2017 (2017 TJBW)
Spetember 3-6, 2017, Tainan, Taiwan

Preparation and Isolation of Cage-like Oligosilsesquioxane (POSS) Containing Carboxyl Side-chain Groups

Jiahao Liu[1] and Yoshiro Kaneko*,[1]

Abstract

Silsesquioxanes (SQs) have attracted much attention in the research fields of materials science. Since SQs contain siloxane bond frameworks and the various organic side-chain groups, they indicate high thermal stabilities and the remarkable compatibilities with organic materials such as polymers. In particular, soluble SQ compounds containing reactive side-chain groups can afford the hybrid materials connected with organic materials by covalent bond. Among these reactive-group-containing SQs, there are only a few synthetic examples of SQs with acidic groups, such as carboxyl side-chain groups, because carboxyl-group-containing organotrialkoxysilanes as starting materials are unstable. So far, as a few examples of soluble carboxyl-group-containing SQs, we have reported the preparation of rod-like polySQs by the hydrolytic condensation of 2-cyanoethyltriethoxysilane using aqueous NaOH[1)] and the modification reaction of amino-group-containing rod-like polySQs with succinic anhydride.[2)] On the other hand, to obtain a cage-like oligoSQ (POSS) containing such side-chain groups, it is necessary the modification reaction.[3), 4)]

In this study, to obtain a POSS containing carboxyl side-chain groups by hydrolytic condensation method, we investigated the reaction of 3-(triethoxysilyl)propyl succinic anhydride (TESPSA) using aqueous tetra-*n*-butylammonium hydroxide ((*n*-Bu)$_4$N·OH) as a catalyst. Then, POSS octamer (T_8-POSS) was isolated by treatment with clay mineral.

The preparation of SQs containing carboxyl side-chain groups was performed by the following procedure: (*n*-Bu)$_4$N·OH was added to TESPSA with stirring and this solution was further stirred for 2 h at room temperature. Then, the solution was heated (*ca*. 50-60^{o}C) in an open system until the solvent was completely evaporated. After the resulting crude product was maintained at 100^{o}C for *ca*. 2 h, acetone was added to this product at room temperature. Then, this solution including (*n*-Bu)$_4$N·OH was neutralized by adding aqueous HCl and this solution was evaporated. After acetone was added again to the resulting product, soluble-part was isolated by filteration and this solution was evaporated. Then, the resulting solid product was washed with chloroform and dried under reduced pressure to yield SQ containing carboxyl side-chain groups (Scheme 1a). The ^{29}Si NMR spectrum of the product in DMSO-*d*$_6$ indicated that the product was a mixture of POSSs as main products and SQs of unknown structures as minor products.

Therefore, we investigated the isolation of T_8-POSS by adsorption/desorption to a clay mineral. This was performed by the following procedure: After the SQ mixure obtained by the aforementioned procedure and Montmorillonite as a clay mineral were mixed in water, the resulting suspension was stirred at room temperature and the insoluble-part was collected by filtration. Then, acetone was added to the resulting solid product and the acetone-soluble-part was corrected by filtration. Finally, the resulting solution was evaporated and dried under reduced pressure to obtain the product (Scheme 1b). It was confirmed that the product was only T_8-POSS by the ^{29}Si NMR spectrum.

References

1) H. Toyodome, Y. Kaneko, K. Shikinaka, and N. Iyi, *Polymer*, **53**, 6021 (2012).

2) Y. Kaneko and N. Iyi, *Z. Kristallogr*., **222**, 656 (2007).

3) K. Tanaka, F. Ishiguro, and Y. Chujo, *J. Am. Chem. Soc.*, **132**, 17649 (2010).

4) A. Boulanger, G. Gracy, N. Bibent, S. Devautour-Viont, S. Clément, and A. Mehdi., *Eur. J. Inorg. Chem.*, 143 (2012).

[1]Graduate School of Science and Engineering, Kagoshima University, Kagoshima, Japan

Taiwan-Japan Bilateral Workshop 2017 (2017 TJBW)

September 3-6, 2017, Tainan, Taiwan

Preparation of tough hybrid hydrogels using water-soluble cyclotetrasiloxane and POSS containing polymerizable side-chain groups as cross-linkers

Makoto Yanagie[1] and Yoshiro Kaneko*,[1]

Abstract

Hydrogels are biofriendly because they are solid materials that can contain abundant water inside them. Therefore, they are used as soft contact lenses and water-absorbing materials for disposable diapers. However, hydrogels are usually fragile. Therefore, the preparation of tough hydrogels is important for their applications. At the beginning of this century, some tough hydrogels have been developed, *e.g.*, slide-ring gel,[1)] nanocomposite gel,[2)] double-network gel,[3)] and tetra-PEG gel.[4)]

On the other hand, we recently found that a single-structured (*cis-trans-cis*) cationic (ammonium-group-containing) cyclotetrasiloxane (**Am-CyTS**)[5)] and POSS (**Am-POSS**)[6)] were successfully prepared by the hydrolytic condensation of 3-aminopropyldiethoxymethylsilane and 3-aminopropyltrimethoxysilane, respectively, using aqueous trifluoromethanesulfonic acid (HOTf) as a catalyst.

In this study, we prepared polymerizable-group-containing cyclotetrasiloxane (**CyTS-MNa**) and POSS (**POSS-MNa**) from **Am-CyTS** and **Am-POSS**, respectively. In addition, we investigated the preparation of tough polyacrylamide (PAAm) hybrid hydrogels using **CyTS-MNa** and **POSS-MNa** as cross-linkers, and evaluated the mechanical properties of the resulting hybrid hydrogels.

First, **CyTS-MNa** and **POSS-MNa** were prepared by the reaction of **Am-CyTS** and **Am-POSS** with maleic anhydride, followed by neutralization with NaOH methanol solution. Then, the PAAm hybrid hydrogels were prepared by free radical polymerization of acrylamide and the resulting cross-linkers (**CyTS-MNa** and **POSS-MNa**) in degassed water under Ar atmosphere. These hybrid hydrogels indicated flexible nature and were not destroyed in the strain of more than 97%.

References

1) Y. Okumura and K. Ito, *Adv. Mater.*, **13**, 485 (2001).
2) K. Haraguchi and T. Takehisa, *Adv. Mater.*, **14**, 16 (2002).
3) J. P. Gong, Y. Katsuyama, T. Kurokawa, and Y. Osada, *Adv. Mater.*, **15**, 1155 (2003).
4) T. Sakai, T. Matsunaga, Y. Yamamoto, C. Ito, R. Yoshida, S. Suzuki, N. Sasaki, M. Shibayama, and U. Chung, *Macromolecules*, **41**, 5379 (2008).
5) S. Kinoshita, S. Watase, K. Matsukawa, and Y. Kaneko, *J. Am. Chem. Soc.*, **137**, 5061 (2015).
6) Y. Kaneko, M. Shoiriki, T. Mizumo, *J. Mater. Chem.*, **22**, 14475 (2012); K. Imai and Y. Kaneko, *Inorg. Chem.*, **56**, 4133 (2017).

[1]Graduate School of Science and Engineering, Kagoshima University, Kagoshima, Japan